Published in final edited form as:
FEBS Lett. 2012 March 9; 586(5): 596–602. doi:10.1016/j.febslet.2011.12.014.

Redox Properties of Tyrosine and Related Molecules[1]

Jeffrey J. Warren, **Jay R. Winkler**, and **Harry B. Gray***
Beckman Institute, California Institute of Technology, Pasadena, CA 91125

Abstract

Redox reactions of tyrosine play key roles in many biological processes, including water oxidation and DNA synthesis. We first review the redox properties of tyrosine (and other phenols) in small molecules and related polypeptides, then report work on (H20)/(Y48)-modified *Pseudomonas aeruginosa* azurin. The crystal structure of this protein (1.18 Å resolution) shows that H20 is strongly hydrogen bonded to Y48 (2.7–2.8 Å tyrosine-O to histidine-N distance). A firm conclusion is that proper tuning of the tyrosine potential by a proton-accepting base is critical for biological redox functions.

Keywords

electron transfer; tyrosine; tyrosyl radical

1. Introduction

Nature employs many different redox cofactors that promote long-range electron transfer [1]. Few cofactors are available, however, that can carry out redox chemistry at potentials near or above 1 V versus NHE. Charge transport at these high potentials is required for key biological transformations such as water oxidation and C-H bond activation. Heme iron, copper, and iron sulfur clusters are common redox “way stations” but they are typically limited to low potentials (less than about 400 mV versus NHE) [2]. Several amino acids have been implicated in high-potential redox catalysis, but the main players are tyrosine (YOH) and tryptophan (W).

Interest in enzymes that use tyrosyl radicals (YO•) in redox catalysis has spurred investigations of a wealth of small molecule and protein-based models. Natural enzymes that use the YOH/YO• redox couple include photosystem II [3], ribonucleotide reductases [4] cytochrome *c* oxidase and related oxygen reductases [5], galactose oxidase [6], prostaglandin synthase [7], and a fatty acid oxygenase [8]. Furthermore, YOH oxidation products are implicated in disease states related to oxidative stress [9]. While we know that many enzymes use YOH in catalysis or long-range electron transfer (ET), we know relatively little about its actual properties within a given enzymatic system. This review focuses on model investigations of tyrosine oxidations in chemistry and biology, including a

[1]Dedicated to the memory of Antonio Xavier, an outstanding scientist and dear friend.

hbgray@caltech.edu.

preliminary report of our work on designing proteins containing redox active units that mimic those found in Nature.

2. Materials and methods

2.1 Protein isolation and purification

The plasmid encoding for H20/Y48 azurin was generated using the Stratagene Quikchange protocol. Protein was expressed as previously described [10]. It should be noted that H20/Y48 azurin is sensitive to pH, precipitating when the pH is below 7.5. Thus, protein was isolated as previously described, except solutions were kept at pH 8.5. Protein was exchanged into 10 mM diethanolamine (DEA)•HCl, pH 9.5 and purified on Q-Sepharose using a NaCl gradient. Protein purity was confirmed by SDS-PAGE and electrospray ionization mass spectrometry.

2.2 Crystal growth, manipulation and x-ray data collection

Cu^{II} azurin (~20 mg/mL) in 10 mM DEA•HCl was mixed with an equivalent volume of well solution containing 25–30% of poly(ethylene glycol) (PEG) 4000, 100 mM lithium nitrate, 10 mM copper sulfate and 100 mM Tris•HCl, pH 8. Crystals suitable for x-ray diffraction were grown using sitting drop vapor diffusion [10]. The drops were allowed to equilibrate against 0.25 mL of well solution over 5 days, by which time plate-like crystals of H20Y48 azurin were obtained. Diffraction data were collected at the Stanford Synchrotron Radiation Laboratory (SSRL) beamline 12-2. The structure was solved by molecular replacement and then refined to the resolution limit from scaling/merging statistics. The coordinates of the structure (1.18 Å resolution) have been deposited in the Protein Data Bank (PDB ID 3U25) (Table[1]).

3. Discussion

The redox chemistry of YOH is inherently “proton-coupled,” meaning that changes in electron inventory are accompanied by changes in proton content. These H^+/e^- transfers are collectively called “proton-coupled electron transfer (PCET).” PCET has come to be known by many different names [11] and full treatment of this nomenclature is beyond the scope of this review. The typical starting point for understanding ET is semiclassical theory (eqn 1) [12] which describes the dependence of intramolecular rate constants on three parameters: the reaction driving force ($-\Delta G°$); the reorganization energy (λ); and the electronic coupling between reactant and products at the transition state nuclear configuration (H_{AB}). Importantly, we are still seeking understanding of key parameters in eqn 1, $-\Delta G°$ and λ, most especially for reactions within and between polypeptides.

$$k_{ET} = \sqrt{\frac{4\pi^3}{h^2 \lambda k_B T}} H_{AB}{}^2 \exp\left(\frac{-(\Delta G° + \lambda)^2}{4\lambda k_B T}\right) \quad (1)$$

The zero-order Born-Oppenheimer approximation that decouples electron and nuclear motions in semiclassical ET theory (eqn. 1) is absent (along at least one coordinate) in PCET reactions. Marcus noted that eq. 1 results when the potential energy along the reaction coordinate is parabolic, as with vibrational or pseudo-vibrational motion. For perspectives on the applicability of semiclasical theory to atom transfers see references [13] and [14]. When bonds are made or broken along the reaction coordinate, simple Born-Oppenheimer separability is lost, the potential energy cannot be described by intersecting parabolic surfaces, and eqn. 1 need not apply. Theoretical models for PCET reactions have been proposed in which rate constants depend on an intrinsic-barrier parameter that resembles the

reorganization parameter (λ) of eqn. 1 [15]. Experimentalists frequently employ models of this type in attempts to understand the driving force dependence of PCET reactions. Since the *ad hoc* parameters extracted in these studies are not the same as ET λ values (eqn. 1), we suggest that a different symbol (γ) should be used to denote the intrinsic barriers associated with PCET reactions, including biologically important cases involving tyrosine and related phenols. We anticipate that continued experimental and theoretical investigations of PCET processes will produce a conceptual framework that does not violate any of the well-established principles of semiclassical ET theory.

We begin our discussion with an introduction to the solution chemistry of phenols and tyrosine. We then consider the mechanisms that have been proposed for reactions involving small molecule models. Next, we turn to investigations of YOH oxidation/reduction in polypeptides. Finally, we discuss work on designed model systems that have shed light on tyrosine redox chemistry.

3.1 Solution thermochemistry

The Pourbaix diagrams reported by Harriman [16] provide a starting point for discussions of the solution redox chemistry of tyrosine and related phenols. They give tyrosine reduction potentials across all biologically relevant pH values that are in good agreement with those from pulse radiolysis experiments [17]. Electrochemical [18] and pulse radiolysis [19] measurements of the tyrosyl/tyrosinate or phenoxyl/phenolate couples complement studies of the H^+/e^- neutral/radical. An estimate of the pKa of the tyrosyl radical cation in aqueous solution [20] completes the thermodynamic square scheme shown in Figure 1. Such schemes are useful for predicting the course of reactions involving reagents that can donate or accept H^+ and e^- [21]. The free energy for $X{-}H \rightarrow X^{\bullet} + H^{\bullet}$ bond homolysis in solution (bond dissociation free energy or BDFE) can be calculated using eqn. 2 as described elsewhere [21,22].

$$\mathrm{BDFE\,(kcal\,mol^{-1})} = 1.37\mathrm{p}K_{\mathrm{a}} + 23.0E^{\circ} + C_{\mathrm{G}} \quad (2)$$

Aqueous thermochemistry is a good starting point for understanding redox reactions of tyrosine, but it provides only a qualitative picture of such reactions in polypeptides. Electrochemical and pulse radiolysis studies of di- and tri-amino acid units indicate that the redox chemistry of tyrosine can be modulated when in a polypeptide [23], but these are still far from native systems. The dielectric environment of any redox cofactor has a great impact on its reduction potential and therefore on $-\Delta G^{\circ}$, a key component of the rate of ET (eqn. 2). As an illustration of this point, we take oxidation of 2,4,6-tri-tertbutylphenol (^{t}Bu$_3$PhOH) in water and acetonitrile as a prototypical example (Figure 2). Note that we choose this as an example because complete thermodynamic cycles are available in ethanol/water and in MeCN. In ethanol/water $E(^t\mathrm{Bu_3PhOH}^{\bullet+/0})$ = 1.28 V *vs*. NHE as derived from simulations of irreversible voltammograms [24], and 1.2 V *vs*. $Cp_2Fe^{+/0}$ in MeCN [25] (1.8 V versus NHE using one common conversion, [26]). The pK_a of this phenol is 13 in ethanol/water, but 28 in MeCN. In contrast, the homolytic bond strengths only change by 3 kcal mol^{-1} from water to MeCN. While we are unable to make *quantitative* predictions of redox potentials of tyrosine within proteins, the *qualitative* conclusion that it is more difficult to generate charged species in a low dielectric medium still holds. On the other hand, bond homolysis does not generate charged species. The thermodynamic data underscore a key component of the reactivity of tyrosine that we will return to below: oxidation and reduction of tyrosine occur with loss and gain of $H^+ + e^-$ in all but extreme cases.

3.2 Small molecule models for tyrosine oxidation

Small molecule models have been reported that probe the proton-coupled oxidation of tyrosine. Hammarström and co-workers have investigated photosystems where tyrosine is covalently linked to a Ru^{II}-tris(diimine) photosensitizer (Figure 3) [27,28] and Nocera has reported analogous photosystems where Re^{I} is the photosensitizer [29]. In both of these systems electron transfer is intramolecular (YOH → Ru^{III}) and proton transfer is intermolecular (H^+ to water/buffer). Interestingly, relatively high reorganization parameters (γ, see above) have been estimated for these reactions (γ > 1.2 eV for ET to Ru and H^+ loss to solvent). Interestingly, the rate constants for oxidation of tyrosine in these models show an unusual pH dependence [30] that has been the source of controversy [31–33]. The origin of this pH dependence has not been resolved.

Solution electrochemical investigations of phenol oxidation where the proton is transferred to an exogenous base (e.g., water, buffer or nitrogen heterocycles) and the electron is transferred to an outer-sphere oxidant or electrode also have been reported. In many ways these reactions are an outgrowth of decades of work on free radical reactions of phenols and related compounds [34] where $H^+ + e^-$ are transferred from phenol (PhOH) to a single acceptor (e.g. PhOH + $R^\bullet$ → $PhO^\bullet$ + RH). In key experiments, Linschitz observed that addition of organic bases to solutions of phenol in acetonitrile facilitates phenol oxidation by excited state oxidants [35]. Likewise, in aqueous solution addition of pyridine [36] facilitates electrochemical oxidation of phenol or ascorbate/quinones. Hammarström [30] and Stanbury [31] have reported phenol oxidation studies where flash-generated $Ru(bpy)_3^{3+}$ or $IrCl_6^{2-}$, respectively, acts as the oxidant and water or buffer is the proton acceptor. Costentin and Savéant have extensively studied electrochemical phenol oxidation where water or buffer acts as proton acceptor [24,37,38]. These workers find that phenol oxidation at an electrode has γ closer to 0.5 eV as determined by varying the driving force for outer-sphere oxidation with proton loss to unbuffered water. In related experiments, Meyer and Thorp have used indium tin oxide electrodes to study electrocatalytic phenol oxidations by $M(bpy)_3^{3+}$ (M = Ru, Os) complexes [39].

Mayer and co-workers have reported outer-sphere oxidation of a series of hydrogen bonded phenol systems in acetonitrile solution (Figure 4) [40–42]. In these systems proton transfer is intramolecular and electron transfer is intermolecular. While these systems may not be good biological mimics, they allow for systematic variation of the oxidant and the proton-accepting base in the H^+/e^- oxidation of phenols. In another recent example [43], the proton transfer distance was varied, allowing for experimental tests of theoretical predictions of proton-coupled electron transfer [15]. Mayer's work suggests that redox reactions of H-bonded phenol models are associated with large γ values (over 2 eV in some cases for ET self-exchange coupled to intramolecular proton transfer). These γ values were obtained by measuring rate constants as a function of driving force and fitting the data using semiclassical ET theory (eqn. 1) [29]. More importantly, these studies provide a very clear example of how a base can affect phenol reduction potentials in a low dielectric environment (the potentials are more than 0.5 V lower than those of the analogous $^tBu_3PhOH^{\bullet+/0}$ couple). Costentin and Savéant also have studied these (and related) phenols by electrochemistry [44], including a case in which phenol oxidation was proposed to occur via an intermolecular proton relay [45].

3.2.1 Mechanisms of tyrosine/phenol oxidations—Three limiting ways to oxidize phenols to phenoxyl radicals are: (1) stepwise oxidation then deprotonation; (2) stepwise deprotonation, then oxidation; and (3) concerted oxidation/deprotonation. As noted above, tyrosine undergoes $1e^-$ oxidation or deprotonation only under forcing conditions because of its high pK_a and high reduction potential in a low dielectric environment, as a protein active

site. In general, the above examples implicate concerted transfer of $H^+ + e^-$ (= $H^\bullet$) as the primary mechanism of phenol oxidation. The clearest mechanistic illustrations come from Costentin and Savéant who used electrochemical simulations [37] and from Mayer's thermodynamic arguments [40]. Take, for example, the degenerate self-exchange reaction between ^{t}Bu$_3$PhOH and ^{t}Bu$_3$PhO$^\bullet$ (Figure 5), where the free energy change for initial ET or proton transfer (PT) is the same, 43 kcal mol^{-1}; and the self-exchange barrier is 15.7 kcal mol^{-1} [46]. Thus, the self-exchange reaction is not likely to proceed via initial ET or PT because even the *ground state* free energy change for those steps is well above the observed barrier. Indeed, it would appear from thermodynamic and kinetics analyses that tyrosine/phenol oxidation occurs via loss of $H^+ + e^-$ in a single step.

3.3 Peptide model systems

Pulse radiolysis and electrochemical experiments on YOH in di- and tri-peptides were mentioned above [23]. Several studies of ET between YOH and $W^{\bullet+}$ radicals generated from reaction with $N_3^{\bullet-}$ using pulse radiolysis have been reported, some involving YOH-W dipeptides [47], while others employed more complex polypeptides with W and YOH separated by one or more amino acids [48]. It has been proposed that systems where W and YOH are separated by a polyproline spacer (Figure 6, top) [49,50] have distance decay constants (β) that are smaller than those documented for Ru-modified proteins [51]. It is our view, however, that the dynamical properties of these polypeptides greatly complicate definitive determinations of distant donor-acceptor couplings [52,53].

More recently, Giese and co-workers have extended work on polyproline-based systems to include models that probe reactions in which YOH is oxidized to YO$^\bullet$ via intramolecular ET (Figure 6, bottom) [54,55]. Multistep tunneling (hopping) involving a redox-active intermediate is the likely mechanism of these reactions [51]. Notably, workers in the Giese lab have employed these model polypeptides to investigate the effects of varying the intermediate amino acid on the hopping rate [56]. While these systems are not specifically geared toward elucidating the redox properties of YOH, they have shed light on the factors that influence hopping rates in biological model systems.

The increasing number of high resolution x-ray structures of enzymes that use YO•/YOH in redox catalysis has spurred the development of protein models that better mimic natural systems. Tommos and co-workers have characterized *de novo* designed 3- and 4-helix bundles containing W or YOH by a variety of techniques [57], including NMR. The solution structure for the 3-helix bundle with an embedded W is shown in Figure 7. [58]. In similar motifs, Tommos has investigated the electrochemical responses of phenol analogues that have been introduced by coupling mercaptophenols to a cysteine residue [59], and she and co-workers are currently studying the redox properties of 3-helix bundles where an embedded tyrosine in each protein is positioned near a proton-accepting base [60].

Barry and co-workers have reported tyrosine-containing peptides that fold in a β-hairpin motif [61]. Although the behavior of tyrosine in this β-hairpin is similar to that in water, it is apparent from electrochemical studies that protonation/deprotonation of nearby amino acids can have a substantial influence on its redox properties [62].

We turn now to recent investigations in our laboratory on multistep electron tunneling (hopping) in modified natural proteins. We have shown that long-range Cu^I oxidation in *Pseudomonas aeruginosa* Re^I(H124)(W122)-azurin is greatly accelerated by hole hopping through tryptophan [63], but we have not been able to observe YOH-assisted hopping in related protein models. Photogenerated YO• radicals in modified azurins have been observed by EPR [64], however, hopping to generate Cu^{II} is not implicated [65,66]. High potential Re^{II} oxidants were used to generate those YO$^\bullet$ radicals and kinetic parameters

could not be extracted. What we have learned from this work is that fine tuning of the reduction potentials of candidate redox intermediates is absolutely critical for hopping function, and for tyrosine such tuning may be achieved by installing a basic amino acid that can hydrogen bond to the YOH proton in a modified protein. Our current investigations are focused on modified azurins where tyrosine is hydrogen bonded to His, Asp or Glu.

We start with a robust protein in which all YOH and W residues have been replaced with phenylalanine, which we call “all-Phe” azurin. Using Rosetta software [67], we surveyed candidates where YOH and His could be introduced near each other (Sheffler, W., Tinberg, C.E. Warren, J.J. Gray, H.B. and Baker, D.A. *work in progress*). Among these all-Phe azurin candidates, one that stood out as particularly attractive was the His20/Tyr48 protein, which we expressed and purified by standard methods. The visible absorption spectrum of the modified protein is identical with that of native azurin (the signature S-Cys to Cu^{II} charge transfer band maximum is at 630 nm).

Importantly, the predicted YOH···His hydrogen bonding interaction is present in the His20/Tyr48 protein (Figure 8). The O···N distance, which is 2.7–2.8 Å based on two molecules in the asymmetric unit, is similar to those in small molecule models where the phenolic oxygen is strongly hydrogen bonded to a nitrogen base [40]. The His-NH is also involved in a weak hydrogen bonding interaction (3.0–3.1 Å) with the backbone carbonyl of the adjacent Thr19. The protein backbone at position 20 is in a different conformation than in other azurin structures, presumably to accommodate the non-conservative Ile→His mutation and the YOH···His hydrogen bond. The protein also shows decreased stability at pH values below 7.5, likely due to protonation of His20, which is located in the hydrophobic core. Our work with the His20/Tyr48 model indicates that engineering redox active YOH into native protein scaffolds can provide better models of natural systems, but challenges such as protein destabilization are vital considerations.

4. Concluding remarks

We have reviewed redox reactions of tyrosine and related phenols ranging from small molecule models in organic solvents to models from our lab that were built within native protein scaffolds. All these investigations share a common goal, namely elucidation of the factors that govern the electron transfer chemistry of tyrosine in biological redox machines.

Work on both small molecule and macromolecular systems indicates that a base near the phenolic proton tunes the $YO^{\bullet}$/YOH reduction potential and also keeps the proton near the YO• radical. Examination of x-ray structures shows that enzymes that use YOH as a redox way station typically place a proton-accepting group near the phenolic proton thereby ensuring that both H^+ and e^- are available to reactions. While a small molecule model can be built with and one of a wide variety of bases (amines, pyridines, imidazoles, carboxylic acids, etc.), natural systems normally employ one of three amino acids (His, Asp, Glu). In proteins where $YO^{\bullet}$ participates in catalysis (e.g. cytochrome *c* oxidase), the redox active YOH placed near a reactive substrate likely serves as a (net) donor/acceptor of $H^{\bullet}$.

An important conclusion is that concerted H^+/e^- loss is a common feature of tyrosine oxidation. Electrochemical experiments have shown that sequential deprotonation, then ET, can be operative in solution when sufficiently strong bases ($pK_a \geq 10$) are present. Even stronger bases could be needed to deprotonate protein-embedded tyrosines. To the best of our knowledge, the radical cation, $YOH^{\bullet+}$, has not been observed in studies of YOH oxidations. Conversely, reduction of $YO^{\bullet}$ is more likely to proceed via initial ET or via a concerted mechanism to avoid production of $YOH^{\bullet+}$. It is interesting to note that in order to maintain high potentials in multistep ET pathways, oxidation of YOH and reduction of $YO^{\bullet}$ probably both proceed via a concerted mechanism; oxidation is concerted to avoid high

energy intermediates and reduction is concerted because the free energy change for H^+/e^- addition to $YO^\bullet$ is higher than $E°(YO^{\bullet/-})$.

A great deal of the work on small molecule systems has focused on the reorganization parameter (γ) for phenol/tyrosine oxidation, but there is little consensus. Different investigators have estimated values of γ ranging from 0.5 to above 2 eV. From a biological perspective, there is no apparent advantage in utilizing cofactors that require extensive nuclear reorganization for function. As illustrated by Roth and Klinman for oxygen reduction by glucose oxidase, the protein matrix can control reorganization parameters [68].

Since the kinetics and thermodynamics of H^+/e^- redox reactions of tyrosine depend so strongly on the nature of its local environment, there is great interest in building models where YOH is positioned in protein environments similar to those of natural systems. Progress in this area has been slow, mainly because control of YOH orientation in relation to nearby groups (including proton acceptors) is not an easy task. Moreover, the redox chemistry of YOH within small protein scaffolds often is complicated by the presence of other ionizable groups, highlighting the difficulty associated with keeping track of protons and electrons in biological macromolecules. Although the experiments are challenging, we believe that the study of suitably designed photosystems by time-resolved spectroscopic methods will provide key insights into the redox chemistry of tyrosine embedded in polypeptides. In such systems, positioning of the photosensitizer relative to tyrosine will be critical for ET function [63,69].

Acknowledgments

We thank Seiji Yamada, Julie Hoy and Jens Kaiser for assistance with x-ray structure determination. Our work is supported by NIH (DK019038 to HBG and JRW; GM095037 to JJW). The Gordon and Betty Moore Foundation supports the Molecular Observatory at Caltech, and NIH and DOE support operation of the Stanford Synchrotron Radiation Laboratory (SSRL) beamline 12-2.

List of abbreviations

ET	electron transfer
PT	proton transfer
YOH	tyrosine
$YO^\bullet$	tyrosyl radical
W	tryptophan
PCET	proton-coupled electron transfer
BDFE	bond dissociation free energy
DEA	diethanolamine
Tris	*tris*(hydroxymethyl)aminomethane

References

1. Bertini, I.; Gray, HB.; Steifel, EI.; Valentine, JS., editors. Biological Inorganic Chemistry: Structure and Reactivity. University Science Books; Herndon, VA: 1994.
2. Taniguchi VT, Sailasuta-Scott N, Anson FC, Gray HB. Thermodynamics of metalloprotein electron transfer reactions. Pure Appl Chem. 1980; 52:2275–2281.
3. Rappaport F, Diner BA. Primary photochemistry and energetics leading to the oxidation of the $(Mn)_4Ca$ cluster and to the evolution of molecular oxygen in Photosystem II. Coord Chem Rev. 2008; 252:259–272.

4. Stubbe J, Nocera DG, Yee CS, Chang MCY. Radical initiation in the class I ribonucleotide reductase: Long-range proton-coupled electron transfer? Chem Rev. 2003; 103:2167–2201. [PubMed: 12797828]
5. Kaila VRI, Verkhovsky MI, Wikström M. Proton-Coupled Electron Transfer in Cytochrome Oxidase. Chem Rev. 2010; 110:7062–7081. [PubMed: 21053971]
6. Whittaker JW. Free Radical Catalysis by Galactose Oxidase. Chem Rev. 2003; 103:2347–2364. [PubMed: 12797833]
7. Tsai AL, Kulmacz RJ. Prostaglandin H synthase: Resolved and unresolved mechanistic issues. Arch Biochem Biophys. 2010; 493:103–124. [PubMed: 19728984]
8. Mukherjee A, Angeles-Boza AM, Huff GS, Roth JP. Catalytic Mechanism of a Heme and Tyrosyl Radical-Containing Fatty Acid α–(Di)oxygenase. J Am Chem Soc. 2010; 133:227–238.
9. Heinecke JW. Oxidized amino acids: culprits in human atherosclerosis and indicators of oxidative stress. Free Radical Bio Med. 2002; 32:1090–1101. [PubMed: 12031894]
10. Lancaster KM, George SD, Yokoyama K, Richards JH, Gray HB. Type-zero copper proteins. Nat Chem. 2009; 1:711–715. [PubMed: 20305734]
11. See: Special Issue on Proton-Coupled Electron Transfer. Chem Rev. 2010; 110:PR1–7099.
12. Marcus RA, Sutin N. Electron transfers in chemistry and biology. Biochim Biophys Acta. 1985; 811:265–322.
13. Marcus RA. Theoretical relations among rate constants, barriers, and Broensted slopes of chemical reactions. J Phys Chem. 1968; 72:891–899.
14. Cohen AO, Marcus RA. Slope of free energy plots in chemical kinetics. J Phys Chem. 1968; 72:4249–4256.
15. Hammes-Schiffer S, Stuchebrukhov AA. Theory of Coupled Electron and Proton Transfer Reactions. Chem Rev. 2010; 110:6939–6960. [PubMed: 21049940]
16. Harriman A. Further comments on the redox potentials of tryptophan and tyrosine. J Phys Chem. 1987; 91:6102–6104.
17. DeFelippis MR, Murthy CP, Faraggi M, Klapper MH. Pulse radiolytic measurement of redox potentials: the tyrosine and tryptophan radicals. Biochemistry. 1989; 28:4847–4853. [PubMed: 2765513]
18. Li C, Hoffman MZ. One-Electron Redox Potentials of Phenols in Aqueous Solution. J Phys Chem B. 1999; 103:6653–6656.
19. Lind J, Shen X, Eriksen TE, Merenyi G. The one-electron reduction potential of 4-substituted phenoxyl radicals in water. J Am Chem Soc. 1990; 112:479–482.
20. Dixon WT, Murphy D. Determination of the acidity constants of some phenol radical cations by means of electron spin resonance. J Chem Soc, Faraday Trans 2. 1976; 72:1221–1230.
21. Warren JJ, Tronic TA, Mayer JM. Thermochemistry of Proton-Coupled Electron Transfer Reagents and its Implications. Chem Rev. 2010; 110:6961–7001. [PubMed: 20925411]
22. Tilset, M. Organometallic Electrochemistry: Thermodynamics of Metal-Ligand Bonding. In: Robert, HC.; Mingos, DMP., editors. Comprehensive Organometallic Chemistry III. Elsevier; Oxford: 2007. p. 279-305.
23. DeFelippis MR, Murthy CP, Broitman F, Weinraub D, Faraggi M, Klapper MH. Electrochemical properties of tyrosine phenoxy and tryptophan indolyl radicals in peptides and amino acid analogs. J Phys Chem. 1991; 95:3416–3419.
24. Costentin C, Louault C, Robert M, Saveant JM. Evidence for Concerted Proton-Electron Transfer in the Electrochemical Oxidation of Phenols with Water As Proton Acceptor. Tri-tert-butylphenol. J Am Chem Soc. 2008; 130:15817–15819. [PubMed: 18975863]
25. Osako T, Ohkubo K, Taki M, Tachi Y, Fukuzumi S, Itoh S. Oxidation Mechanism of Phenols by Dicopper–Dioxygen (Cu_2/O_2) Complexes. J Am Chem Soc. 2003; 125:11027–11033. [PubMed: 12952484]
26. Pavlishchuk VV, Addison AW. Conversion constants for redox potentials measured versus different reference electrodes in acetonitrile solutions at 25°C. Inorg Chim Acta. 2000; 298:97–102.

27. Sjödin M, Styring S, Kermark B, Sun L, Hammarström L. Proton-Coupled Electron Transfer from Tyrosine in a Tyrosine-Ruthenium-tris-Bipyridine Complex: Comparison with $Tyrosine_Z$ Oxidation in Photosystem II. J Am Chem Soc. 2000; 122:3932–3936.
28. Sjödin M, Styring S, Wolpher H, Xu Y, Sun L, Hammarström L. Switching the Redox Mechanism: Models for Proton-Coupled Electron Transfer from Tyrosine and Tryptophan. J Am Chem Soc. 2005; 127:3855–3863. [PubMed: 15771521]
29. Reece SY, Nocera DG. Direct Tyrosine Oxidation Using the MLCT Excited States of Rhenium Polypyridyl Complexes. J Am Chem Soc. 2005; 127:9448–9458. [PubMed: 15984872]
30. Irebo T, Reece SY, Sjoedin M, Nocera DG, Hammarström L. Proton-Coupled Electron Transfer of Tyrosine Oxidation: Buffer Dependence and Parallel Mechanisms. J Am Chem Soc. 2007; 129:15462–15464. [PubMed: 18027937]
31. Krishtalik LI. pH-dependent redox potential: how to use it correctly in the activation energy analysis. Biochim Biophys Acta. 2003; 1604:13–21. [PubMed: 12686417]
32. Costentin C, Robert M, Savéant JM. Concerted Proton–Electron Transfer Reactions in Water. Are the Driving Force and Rate Constant Depending on pH When Water Acts as Proton Donor or Acceptor? J Am Chem Soc. 2007; 129:5870–5879. [PubMed: 17428051]
33. Song N, Stanbury DM. Proton-Coupled Electron-Transfer Oxidation of Phenols by Hexachloroiridate(IV). Inorg Chem. 2008; 47:11458–11460. [PubMed: 19006385]
34. Fischer, H., editor. Landolt-Börnstein New Series. Vol. 18. Springer; Berlin: 1994. Radical Reaction Rates in Liquids. Subvols A–E2
35. Gupta N, Linschitz H, Biczok L. Reduction of triplet C60 by hydrogen-bonded naphthols: concerted electron and proton movement. Fullerene Sci Technol. 1997; 5:343–353.
36. Bonin J, Costentin C, Robert M, Savéant JM. Pyridine as proton acceptor in the concerted proton electron transfer oxidation of phenol. Org Biomol Chem. 2011; 9:4064–4069. [PubMed: 21499600]
37. Bonin J, Costentin C, Louault C, Robert M, Routier M, Savéant JM. Intrinsic reactivity and driving force dependence in concerted proton–electron transfers to water illustrated by phenol oxidation. Proc Nat Acad Sci USA. 2010; 107:3367–3372. [PubMed: 20139306]
38. Costentin C, Louault C, Robert M, Savéant JM. The electrochemical approach to concerted proton-electron transfers in the oxidation of phenols in water. Proc Nat Acad Sci USA. 2009; 106:18143–18148. [PubMed: 19822746]
39. Fecenko CJ, Thorp HH, Meyer TJ. The Role of Free Energy Change in Coupled Electron-Proton Transfer. J Am Chem Soc. 2007; 129:15098–15099. [PubMed: 17999500]
40. Rhile IJ, Markle TF, Nagao H, DiPasquale AG, Lam OP, Lockwood MA, Rotter K, Mayer JM. Concerted Proton-Electron Transfer in the Oxidation of Hydrogen-Bonded Phenols. J Am Chem Soc. 2006; 128:6075–6088. [PubMed: 16669677]
41. Markle TF, Rhile IJ, DiPasquale AG, Mayer JM. Probing concerted proton-electron transfer in phenol-imidazoles. Proc Natl Acad Sci U S A. 2008; 105:8185–8190. [PubMed: 18212121]
42. Markle TF, Mayer JM. Concerted proton-electron transfer in pyridylphenols: the importance of the hydrogen bond. Angew Chem, Int Ed. 2008; 47:738–740.
43. Markle TF, Rhile IJ, Mayer JM. Kinetic Effects Of Increased Proton Transfer Distance On Proton-Coupled Oxidations Of Phenol-Amines. J Am Chem Soc. 2011; 133:17341–17352. [PubMed: 21919508]
44. Costentin C, Robert M, Savéant JM. Electrochemical and Homogeneous Proton-Coupled Electron Transfers: Concerted Pathways in the One-Electron Oxidation of a Phenol Coupled with an Intramolecular Amine-Driven Proton Transfer. J Am Chem Soc. 2006; 128:4552–4553. [PubMed: 16594674]
45. Costentin C, Robert M, Savéant JM, Tard C. H-bond relays in proton-coupled electron transfers. Oxidation of a phenol concerted with proton transport to a distal base through an OH relay. Phys Chem Chem Phys. 2011; 13:5353–5358. [PubMed: 21225050]
46. Warren JJ, Mayer JM. Predicting organic hydrogen atom transfer rate constants using the Marcus cross relation. Proc Natl Acad Sci USA. 2010; 107:5282–5287. [PubMed: 20215463]
47. Prütz WA, Land EJ. Reaction of azide radical with amino-acids and proteins. Int J Radiat Biol. 1979; 36:75–83.

48. Prütz WA, Siebert F, Butler J, Land EJ, Menez A, Montenay-Garestier T. Charge transfer in peptides: Intramolecular radical transformations involving methionine, tryptophan and tyrosine. Biochim Biophys Acta. 1982; 705:139–149.
49. DeFelippis MR, Faraggi M, Klapper MH. Evidence for through-bond long-range electron transfer in peptides. J Am Chem Soc. 1990; 112:5640–5642.
50. Mishra AK, Chandrasekar R, Faraggi M, Klapper MH. Long-range electron transfer in peptides. Tyrosine reduction of the indolyl radical: reaction mechanism, modulation of reaction rate, and physiological considerations. J Am Chem Soc. 1994; 116:1414–1422.
51. Gray HB, Winkler JR. Electron flow through metalloproteins. Biochim Biophys Acta. 2010; 1797:1563–1572. [PubMed: 20460102]
52. Butler J, Land EJ, Prütz WA, Swallow AJ. Charge transfer between tryptophan and tyrosine in proteins. Biochim Biophys Acta. 1982; 705:150–162.
53. Gray HB, Winkler JR. Long-range electron transfer. Proc Natl Acad Sci U S A. 2005; 102:3534–3539. [PubMed: 15738403]
54. Cordes M, Jacques O, Köttgen A, Jasper C, Boudebous H, Giese B. Development of a Model System for the Study of Long Distance Electron Transfer in Peptides. Adv Synth Catal. 2008; 350:1053–1062.
55. Cordes M, Köttgen A, Jasper C, Jacques O, Boudebous H, Giese B. Influence of Amino Acid Side Chains on Long-Distance Electron Transfer in Peptides: Electron Hopping via “Stepping Stones”. Angew Chem Int Ed. 2008; 47:3461–3463.
56. Wang M, Gao J, Muller P, Giese B. Electron Transfer in Peptides with Cysteine and Methionine as Relay Amino Acids. Angew Chem Int Ed. 2009; 48:4232–4234.
57. Tommos C, Skalicky JJ, Pilloud DL, Wand AJ, Dutton PL. Biochemistry. 1999; 38:9495–9507. [PubMed: 10413527]
58. Dai QH, Tommos C, Fuentes EJ, Blomberg MRA, Dutton PL, Wand AJ. Structure of a de Novo Designed Protein Model of Radical Enzymes. J Am Chem Soc. 2002; 124:10952–10953. [PubMed: 12224922]
59. Hay S, Westerlund K, Tommos C. Moving a Phenol Hydroxyl Group from the Surface to the Interior of a Protein: Effects on the Phenol Potential and pK_A. Biochemistry. 2005; 44:11891–11902. [PubMed: 16128591]
60. Martínez-Rivera MC, Berry BW, Valentine KG, Westerlund K, Hay S, Tommos C. Electrochemical and Structural Properties of a Protein System Designed To Generate Tyrosine Pourbaix Diagrams. J Am Chem Soc. 2011; 133:17786–17795. [PubMed: 22011192]
61. Sibert R, Josowicz M, Porcelli F, Veglia G, Range K, Barry BA. Proton-Coupled Electron Transfer in a Biomimetic Peptide as a Model of Enzyme Regulatory Mechanisms. J Am Chem Soc. 2007; 129:4393–4400. [PubMed: 17362010]
62. Sibert RS, Josowicz M, Barry BA. Control of Proton and Electron Transfer in de Novo Designed, Biomimetic β Hairpins. ACS Chem Biol. 2010; 5:1157–1168. [PubMed: 20919724]
63. Shih C, Museth AK, Abrahamsson M, Blanco-Rodriguez AM, Di B, Angel J, Sudhamsu J, Crane BR, Ronayne KL, Towrie M, Vlcek A Jr, Richards JH, Winkler JR, Gray HB. Tryptophan-Accelerated Electron Flow Through Proteins. Science. 2008; 320:1760–1762. [PubMed: 18583608]
64. Di Bilio AJ, Crane BR, Wehbi WA, Kiser CN, Abu-Omar MM, Carlos RM, Richards JH, Winkler JR, Gray HB. Properties of Photogenerated Tryptophan and Tyrosyl Radicals in Structurally Characterized Proteins Containing Rhenium(I) Tricarbonyl Diimines. J Am Chem Soc. 2001; 123:3181–3182. [PubMed: 11457048]
65. Winkler JR, Di Bilio AJ, Farrow NA, Richards JH, Gray HB. Electron tunneling in biological molecules. Pure Appl Chem. 1999; 71:1753–1764.
66. Miller JE, Di B, Angel J, Wehbi WA, Green MT, Museth AK, Richards JR, Winkler JR, Gray HB. Electron tunneling in rhenium-modified Pseudomonas aeruginosa azurins. Biochim Biophys Acta. 2004; 1655:59–63. [PubMed: 15100017]
67. Rohl CA, Strauss CEM, Misura KMS, Baker D. Numerical Computer Methods, Part D Method. Enzymol. 2004:66–93.

68. Roth JP, Klinman JP. Catalysis of electron transfer during activation of O2 by the flavoprotein glucose oxidase. Proc Natl Acad Sci USA. 2003; 100:62–67. [PubMed: 12506204]
69. Warren JJ, Ener ME, Winkler JR, Vlcek AA, Gray HB. submitted.

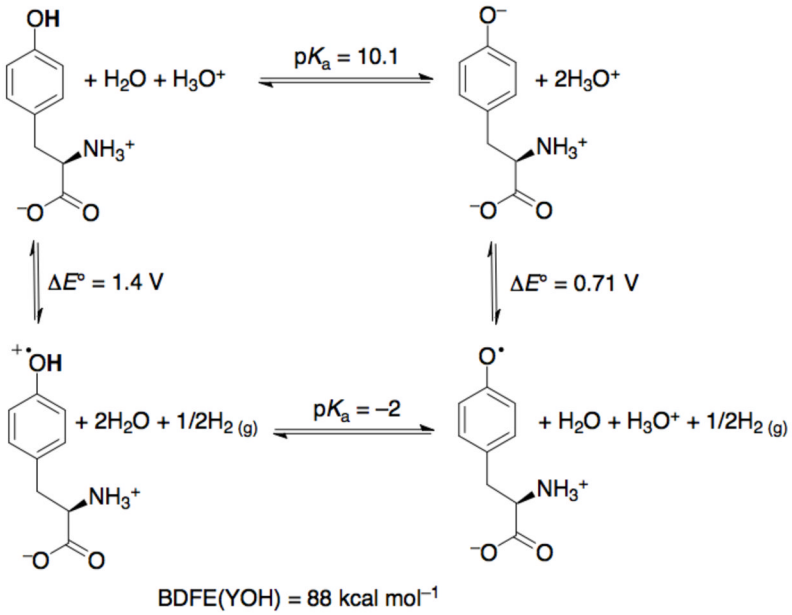

Figure 1.

Thermodynamic cycle for tyrosine in aqueous media. The constant C_G accounts for the free energy to make $H^{\bullet}_{(solv)}$ from $\frac{1}{2}H_2(g)$ such the BDFE corresponds to the chemical reaction $XH \rightarrow X^{\bullet} + H^{\bullet}$.

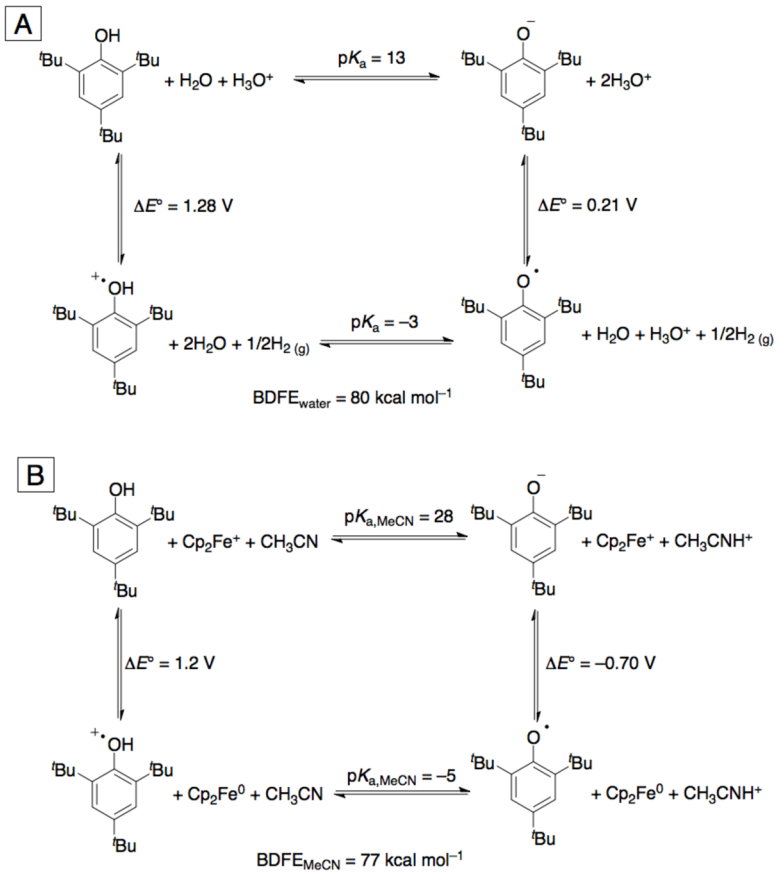

Figure 2.

Thermodynamic cycles for tri-*tert*-butylphenol in (A) ethanol/water and (B) acetonitrile. The constant C_G for (A) is as described in Figure 1. In MeCN (B), the constant C_G relates $CH_3CNH^+ + Cp_2Fe^0$ to $1/2H_2$ and then to $H^\bullet_{(solv)}$ so that the BDFE corresponds to the chemical reaction $XH \rightarrow X^\bullet + H^\bullet$. A derivation and descriptions of the assumptions implicit in this value is given in reference [22].

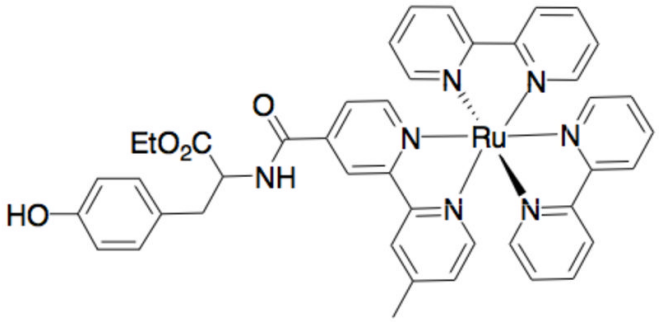

Figure 3.
Ru^{II} photosystem for studying tyrosine oxidation. Flash-generated Ru^{III} is the oxidant. The driving force can be varied by changing the ancillary bipyridine ligands.

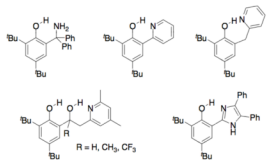

Figure 4.
Small molecule models for phenol oxidation where outer-sphere ET is coupled to intramolecular proton transfer.

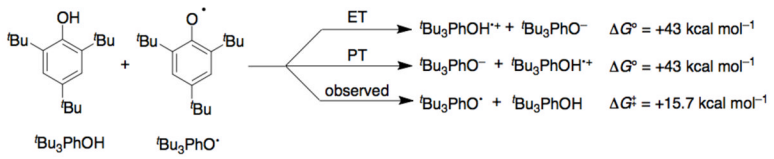

Figure 5.

Pathways for H^+/e^- oxidation of ^{t}Bu$_3$PhOH. $\Delta G°$ is the standard free energy change estimated using data from Figure 2 (MeCN). $\Delta G^‡$ is the barrier calculated from the Eyring equation ($k = (k_BT/h)\exp(-\Delta G^‡/RT)$) for the self-exchange rate constant for H•• exchange.

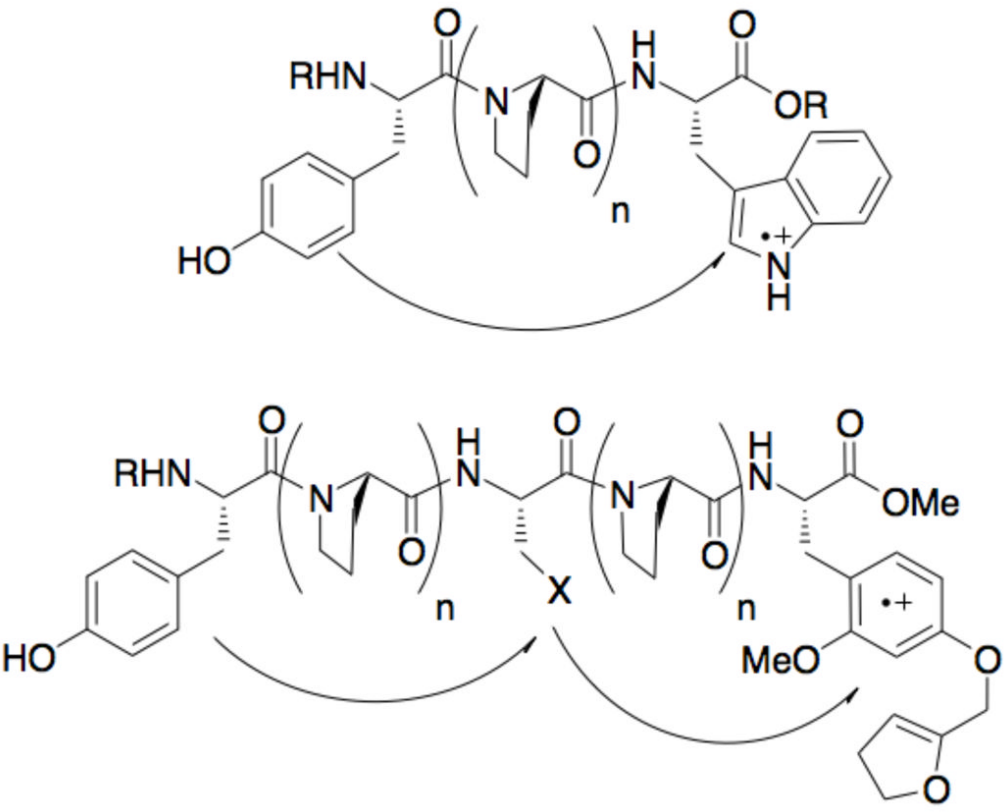

Figure 6.
Polyproline bridged models for studying tyrosine redox chemistry. (top) $W^{\bullet+}$ radicals generated using pulse radiolysis. (bottom) dialkoxyphenylalanine radicals generated using laser-flash techniques. X groups that have been studied include trimethoxyphenylalanine, tryptophan, methionine, alanine and cysteine.

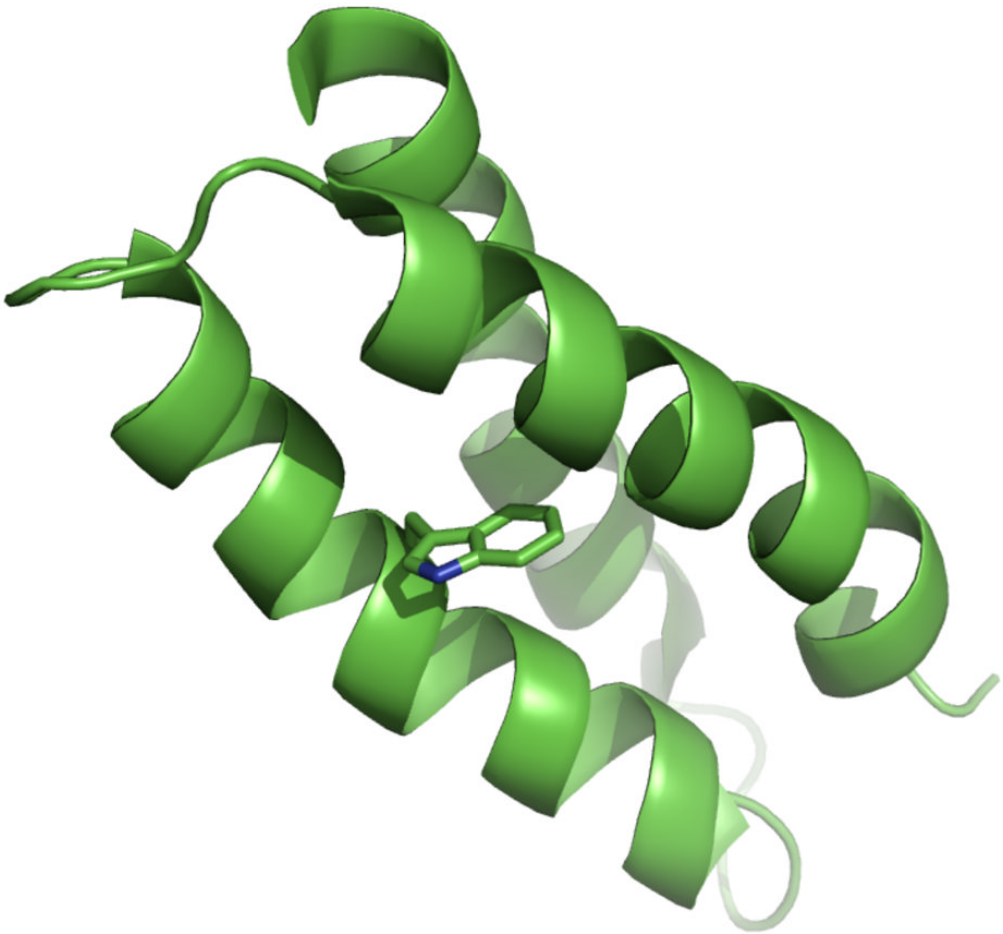

Figure 7.
NMR structure of an α_3W 3-helix bundle: PDB ID 1LQ7. Tryptophan is highlighted.

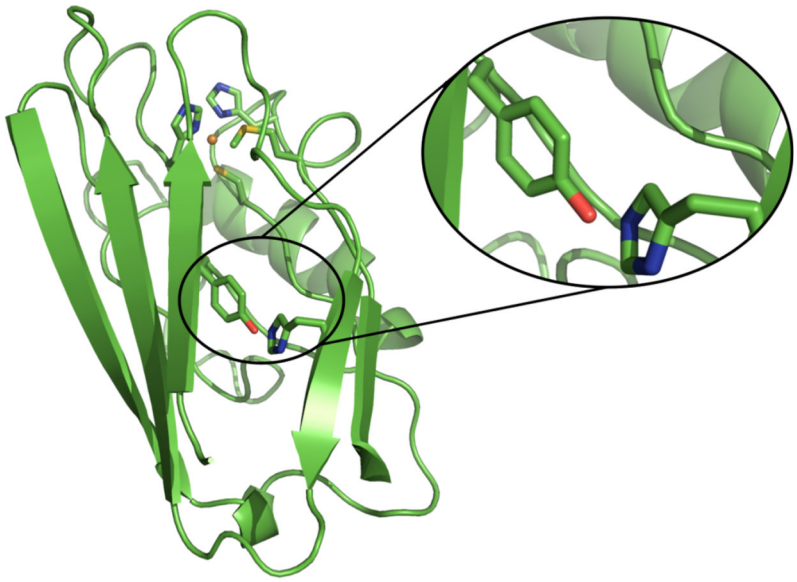

Figure 8.
H20/Y48 azurin structure with a close-up view of the H20···Y48 hydrogen bond.

Table 1

Crystallographic statistics.

	H20/Y48 azurin
Space group	P 2_1 2_1 2_1
A,B,C	48.026, 56.330, 82.910
α,β,γ	90, 90, 90
Observed reflections[a]	262814 (32071)
Unique reflections[a]	70523 (10078)
Completeness[a]	94.9% (84.9%)
R_{obs}[a,b]	4.3% (27.1%)
I/σI[a,c]	15.63 (3.72)
Resolution range	1.18–20.0
High resolution bin	1.182–1.213
R_{free} (e.s.u.)	21.7% (0.047 Å)
$R_{working\ set}$(e.s.u.)	19.5 % (0.048 Å)
Mean B	12.878
RMS deviation: bond lengths	0.029
RMS deviation: bond angles	2.336
Refined amino acids (waters)	254 (277)

[a] Total (outershell).

[b] (SUM(ABS(I(h,i)−I(h))))/(SUM(I(h,i))).

[c] mean of intensity/σI of unique reflections (after merging symmetry-related observations).